Effects of heat release on turbulent shear flows. Part 1. A general equivalence principle for non-buoyant flows and its application to turbulent jet flames

By KATHLEEN M. TACINA AND WERNER J. A. DAHM†

Laboratory for Turbulence and Combustion (LTC), Department of Aerospace Engineering,
The University of Michigan, Ann Arbor, MI 48109-2140, USA

We address the differences observed due to heat release between reacting and non-reacting versions of otherwise identical shear flows under conditions for which buoyancy effects are negligible. The differences considered here result from density changes produced by exothermic reaction, and are shown to be similar to those produced by free-stream density differences in non-reacting flows. The piecewise linear variations of temperature with mole fraction allow the density changes due to exothermic reaction to be related to an equivalent non-reacting flow, in which the temperature of one of the fluids is raised to an effective value determined by the peak temperature and overall stoichiometry. This leads to a general equivalence principle by which the scaling laws for non-reacting flows can be extended to predict effects of heat release by exothermic reaction. This equivalence principle is then applied to axisymmetric turbulent jets, where it leads to a generalized momentum diameter d^+ in which the scaling laws for burning and non-burning jets become identical – it effectively extends the classical momentum diameter d^* of Thring & Newby (1953) and Ricou & Spalding (1961) to exothermic reacting flows. The resulting predicted effects of heat release, in both the near and far fields, show good agreement with experimental data from momentum-dominated turbulent jet diffusion flames. The equivalence principle is then applied to planar turbulent jets, for which it also accurately predicts the observed effects of combustion heat release.

1. Introduction

Proper accounting for the effects of reaction heat release on the properties of turbulent shear flows is an essential bridge between fluid dynamics and combustion science. Studies of mixing without heat release in jets and other shear flows have been used in combustion science since the earliest work of Hottel & Hawthorne (1949) and Hawthorne, Weddel & Hottel (1949). Yet is has been widely observed that density changes due to heat release dramatically alter some of the most fundamental properties of these flows, even under conditions for which buoyancy effects are negligible (e.g. Eickhoff & Lenze 1969). Based on such observations, the relevance of results from flows without heat release to exothermic reacting flows has long been questioned, with some studies concluding that flows with heat release are inherently different from non-burning flows (e.g. Beér & Chigier 1983).

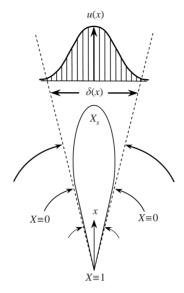† Author to whom correspondence should be addressed.

$u(x)$

$\delta(x)$

X_s

$X \equiv 0$ x $X \equiv 0$

$X \equiv 1$

FIGURE 1. Schematic indicating local outer variables $\delta(x)$ and $u(x)$ that characterize the mean shear at any downstream location x in a turbulent shear flow, in this case a turbulent jet. Within the stoichiometric contour, fluid is typically at mole fractions $X(x,t) > X_s$.

Though many aspects of turbulent shear flows are observed to change with combustion heat release, interest is in practice often focused on entrainment and mixing rates, since these determine such fundamental properties as flame lengths, heat release distributions, induced flow fields, and mutual interference effects. There have been attempts to heuristically account for changes due to heat release on the entrainment and mixing properties of some specific flows (e.g. Eickhoff & Lenze 1969), but to date no fundamentally rooted or generally applicable approach exists to predict the effects of heat release on turbulent shear flows.

There are, of course, many elementary phenomena that can arise in a flow as a consequence of heat release. Among these are changes in the fluid viscosity and diffusivities, which can increase dramatically with temperature and thereby lead, in part, to a large reduction in Reynolds number. However in turbulent flows that remain at sufficiently high Reynolds number, the influence of these molecular transport properties is confined to the smallest scales of motion, and thus plays no direct role in setting the entrainment and mixing rates. With regard to kinematics, there is a volume source field produced by the Lagrangian rate of change in density due to heat release. Typically, however, the resulting induced velocity field is small in comparison with that induced by the underlying vorticity field. As for dynamical effects, heat release generates baroclinic vorticity from interactions of density gradients with both hydrostatic and hydrodynamic pressure gradients. The former, classically termed 'buoyancy effects', can be quite pronounced even in flows without heat release. These are, however, fundamentally different from the heat release effects considered here, which will be present even in the absence of any buoyancy.

Here we will examine the influence of density changes due to heat release on the scaling laws that govern the flow itself. Turbulent shear flows typically grow only relatively slowly with downstream distance x, and for this reason such flows are classically treated as quasi-one-dimensional. Accordingly, local properties of the flow, such as entrainment and mixing rates, are determined by the outer variables

$\delta(x)$ and $u(x)$, namely the length and velocity scales that characterize the local mean shear at any downstream location in the flow, as indicated in figure 1. Consistent with this, the local range of spatial and temporal scales in the flow is characterized by the local outer-scale Reynolds number $Re_\delta(x) \equiv u\delta/\nu$. Scaling laws for δ and u can often be determined by simple dimensional reasoning, and generally depend on the fluid densities even in flows without heat release. When heat release is present, the resulting density changes can therefore be expected to affect the flow through these scaling laws. It is this effect that will be considered herein, and it will be seen that this appears to be the dominant effect of heat release on entrainment and mixing rates, as well as other properties of the flow that are determined by the outer variables, in most high Reynolds number turbulent shear flows when buoyancy is negligible.

There are, in addition, other effects of heat release that go beyond the classical quasi-one-dimensional treatment of turbulent shear flows, and which will not be addressed here. These include, for example, departures from strict self-similarity that arise as a result of lateral variations in the fluid properties due to heat release. Similarly, the increase in viscosity due to heat release can reduce $Re_\delta(x)$ sufficiently to render a flow transitional or even laminar, and such situations also will not be addressed here. Rather, we will confine attention to flows which remain fully turbulent, and develop a general means to understand heat release effects within the classical quasi-one-dimensional treatment of turbulent shear flows. This in turn allows prediction of the resulting effects of heat release on entrainment and mixing rates, flame lengths, and other flow properties determined by the outer-variable scalings.

In §2 we develop a general equivalence principle that relates density changes due to heat release in a reacting flow to an equivalent change in one of the fluid densities in the corresponding non-reacting flow. We then apply this general principle to the far field of axisymmetric turbulent jets in §3, where it leads to a generalized momentum diameter d^+ that unifies the scaling laws for turbulent jets with and without heat release. The predicted effects of heat release are compared with data from momentum-dominated jet flames. The equivalence principle is then applied to planar turbulent jets in §4, and similar comparisons are made of the resulting predicted effects of heat release with measurements in planar turbulent jet flames. In §5, effects due to heat release on the near field of axisymmetric and planar turbulent jets are obtained from this equivalence principle and compared with experimental observations. In §6 we summarize this general equivalence principle and the conditions under which it applies.

2. General equivalence principle

2.1. *Temperature fields in flows without heat release*

Consider first the density field $\rho(\boldsymbol{x}, t)$ created by differences in fluid temperatures in a flow without heat release. For any such adiabatic flow involving two fluids, denoted 0 and 1 respectively at temperatures T_0 and T_1, enthalpy conservation allows the temperature field $T(\boldsymbol{x}, t)$ that results from mixing of the two fluids to be everywhere related to the local mole fraction $X(\boldsymbol{x}, t)$ of fluid 1. If the fluids can be taken as calorically perfect, then

$$T(\boldsymbol{x}, t) = T_0 + (T_1 - T_0)(X(\boldsymbol{x}, t) + \Pi), \tag{1}$$
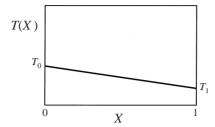
FIGURE 2. Variation of temperature $T(x,t)$ with mole fraction $X(x,t)$ in a non-reacting flow formed by two fluids at temperatures T_0 and T_1, corresponding respectively to mole fractions $X = 0$ and $X = 1$. The linear form of $T(X)$ is indicative of simple mixing without reaction.
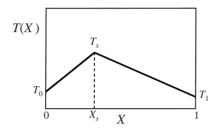

FIGURE 3. Variation of temperature $T(x,t)$ with mole fraction $X(x,t)$ in an exothermic reacting flow, showing stoichiometric temperature T_s at mole fraction X_s. Note that the linear form of $T(X)$ on either side of X_s is indicative of simple mixing, without reaction, of either fluid with stoichiometric products.
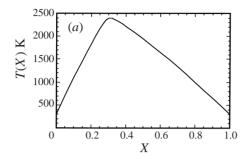
with the nonlinearity in X being

$$\Pi \equiv X(1-X)\left[\frac{\Delta C_p}{C_{p,0}}\right]\left\{\frac{1}{1 + X\left[\Delta C_p/C_{p,0}\right]}\right\}, \qquad (2)$$

as shown schematically in figure 2. The nonlinearity depends on the *molar* specific heat difference $\Delta C_p \equiv C_{p,1} - C_{p,0}$. Unlike mass specific heats, the molar specific heat difference in (2) is typically small, and when this is the case then $T(X)$ will be essentially linear whenever there is simple mixing without heat release between two fluids.

2.2. *Temperature fields in exothermic reacting flows*

Consider now the case when exothermic chemical reactions occur between the two fluids. Attention will be restricted to adiabatic flows, and activation energies that are sufficiently large for the reactions to be confined to a narrow range of mole fractions around the stoichiometric value X_s, where the temperature reaches its peak value T_s. The temperature field $T(x,t)$ can then again be related to the mole fraction field $X(x,t)$. As shown schematically in figure 3, in this case it becomes convenient to equivalently view $T(X < X_s)$ as resulting from simple mixing, without reaction, of fluid 0 at temperature T_0 with stoichiometric products at $X = X_s$ and temperature T_s. Similarly $T(X > X_s)$ can be viewed as resulting from simple mixing of stoichiometric products at temperature T_s with fluid 1 at temperature T_1. From the linearity noted above in the temperature field that results from simple mixing, $T(X)$ in such a reacting flow is thus necessarily piecewise linear, as indicated in figure 3.

This is demonstrated in figure 4(a, b) for adiabatic equilibrium of hydrogen–air chemistry, for which the resulting high temperatures provide a test of the calorically
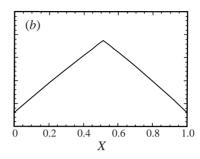
FIGURE 4. (*a*) Adiabatic equilibrium temperature T due to mixing and chemical reaction of pure H_2 (fluid 1) and air (fluid 0), both initially at $300\,K$, shown against the mole fraction X of fluid 1. Results are from detailed thermochemistry, and correspond to several cases in table 1. Even for these relatively high T_{max} and large differences in specific heats, $T(X)$ is nearly linear on either side of X_s. (*b*) Similar to (*a*), but for mixing and reaction of 40% H_2+60% N_2 with air, corresponding to Takagi *et al.* (1981) in table 1. The stoichiometric mole fraction X_s shifts to 0.514 and temperature T_s decreases to $1872\,K$. Due principally to the lower temperatures, $T(X)$ on either side of X_s is even more nearly linear than in (*a*). This piecewise linearity leads to the equivalence principle in figure 5.
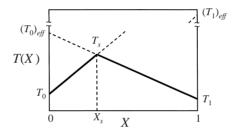

FIGURE 5. Effective fluid temperatures $(T_0)_{eff}$ and $(T_1)_{eff}$ obtained by extrapolating $T(X)$ in figure 3 on either side of the stoichiometric value X_s. Since a linear $T(X)$ is indicative of simple mixing without reaction as in figure 2, wherever $X(\boldsymbol{x}, t) > X_s$, the temperature field $T(\boldsymbol{x}, t)$ in the reacting flow will be the same as that resulting from simple mixing in a non-reacting flow with T_0 replaced by $(T_0)_{eff}$. A similar equivalence holds at $X(\boldsymbol{x}, t) < X_s$ if instead T_1 is replaced by $(T_1)_{eff}$.

perfect gas approximation, and the large differences in specific heats test the significance of the nonlinearity in (2). Even in these cases, $T(X)$ on either side of X_s can be seen to be nearly linear. This piecewise linearity provides the basis for an equivalence between flows with and without reaction heat release.

2.3. *Effective temperatures and densities*

As shown in figure 5, from the piecewise linearity of $T(X)$ in such exothermic reacting flows, wherever $X(\boldsymbol{x}, t) > X_s$ the temperature $T(\boldsymbol{x}, t)$ will be equivalent to that which would result from simple mixing without reaction between an inert fluid 1 at its actual temperature T_1 and density ρ_1, and an inert fluid 0 at an effective elevated temperature $(T_0)_{eff}$ given by

$$(T_0)_{eff} \equiv T_1 + \frac{T_s - T_1}{1 - X_s}, \tag{3a}$$

and hence at a corresponding effective density

$$(\rho_0)_{eff} = \rho_0 \left(T_0 / (T_0)_{eff} \right), \tag{3b}$$

where the effect of molecular weight variations due to chemical reaction are ignored in the density since these are typically small compared with the effect of temperature changes due to heat release (see the Appendix). Both the reacting flow and the fictitious non-reacting flow will have the same temperature fields $T(x,t)$, and thus essentially the same density fields $\rho(x,t)$, wherever $X(x,t) > X_s$.

Similarly, wherever $X(x,t) < X_s$ the temperature $T(x,t)$ in the reacting flow will be equivalent to that produced by mixing without reaction between an inert fluid 0 at its actual temperature T_0 and density ρ_0, and an inert fluid 1 at $(T_1)_{eff}$ given by

$$(T_1)_{eff} \equiv T_0 + (T_s - T_0)/X_s, \tag{4a}$$

with corresponding effective density

$$(\rho_1)_{eff} = \rho_1 \left(T_1/(T_1)_{eff} \right), \tag{4b}$$

where, again, the effects of molecular weight variations on the density are typically much smaller and thus neglected.

When there is significant curvature in $T(X)$ near X_s, then it is appropriate to express T_s in terms of the average slopes as

$$T_s = T_1 + \left\langle -\frac{\mathrm{d}T}{\mathrm{d}X}\bigg|_{X \gg X_s} \right\rangle (1 - X_s), \tag{5a}$$

in $(3a)$, and

$$T_s = T_0 + \left\langle \frac{\mathrm{d}T}{\mathrm{d}X}\bigg|_{X \ll X_s} \right\rangle X_s, \tag{5b}$$

in $(4a)$.

2.4. *Equivalence between reacting and non-reacting flows*

Under these conditions, the density field $\rho(x,t)$ in a reacting flow at values of $X(x,t)$ above (or below) X_s will be the same as that in a fictitious non-reacting flow with the appropriate fluid density replaced by its effective value in $(3b)$ or $(4b)$ and with the other fluid density kept at its true value. Thus the effects of density changes due to heat release on the outer variables in an exothermic reacting flow should be deducible from the scaling laws that apply in the corresponding non-reacting flow by simply replacing the appropriate fluid density with its effective value. Based on the equivalence noted in figure 5, at values of the downstream distance x for which $X(x,t)$ is predominantly above X_s, the scaling laws for the exothermic flow are obtained from those for the corresponding non-reacting flow by replacing ρ_0 with $(\rho_0)_{eff}$ from $(3b)$. Similarly, at x-values for which $X(x,t)$ is predominantly below X_s, the effects of density variations due to heat release would be accounted for by replacing ρ_1 with $(\rho_1)_{eff}$ from $(4b)$ in the scaling laws for the local outer variables $\delta(x)$ and $u(x)$ in the corresponding non-reacting flow.

In the sections that follow, it will be seen that this simple equivalence principle between reacting and non-reacting flows accurately predicts the effects of heat release on the outer variables of turbulent shear flows under conditions for which buoyancy effects are negligible.

3. Heat release effects in axisymmetric turbulent jets

In this section the general equivalence principle from §2 is applied to determine the effects of combustion heat release on axisymmetric turbulent jets. The result-

ing predicted heat release effects are then compared with experimental data from non-buoyant turbulent jet diffusion flames to assess the validity of the equivalence conjectured above between reacting and non-reacting turbulent shear flows.

3.1. *Scaling laws for non-reacting jets*

In the self-similar far field of non-reacting axisymmetric turbulent jets, the outer variables $\delta(x)$ and $u(x)$ are the mean flow width and centreline velocity, as indicated in figure 1. Scaling laws for these can be found by dimensional reasoning in terms of the jet source momentum flux J_0, which is an invariant of the flow, the ambient fluid density ρ_∞, and the downstream distance x as

$$\delta = 0.44\,x, \tag{6a}$$

$$u = 7.3(J_0/\rho_\infty)^{1/2}x^{-1}, \tag{6b}$$

with the scaling constants obtained from experimental data (e.g. Wygnanski & Fiedler 1969). The constant in (6a) gives the full width δ where the mean velocity is 5% of its local centreline value; the constant for other definitions can be obtained from the mean profile.

It is popular to equivalently write (6b) in terms of an 'exit velocity' $u_0 \equiv (J_0/m_0)$, where m_0 is the jet source mass flux, as

$$u/u_0 = 6.5(x/d^*)^{-1} \tag{7}$$

where d^* is the far-field equivalent source diameter, given by

$$d^* \equiv \frac{2m_0}{(\pi\rho_\infty J_0)^{1/2}}. \tag{8}$$

For jets issuing with uniform density and velocity from circular nozzles, d^* reduces to

$$d^* = (\rho_0/\rho_\infty)^{1/2}d_0, \tag{9}$$

where d_0 is the physical source diameter and ρ_0 is the jet fluid density. Thring & Newby (1953) first proposed d^*, called the 'momentum diameter', to account for density differences between the jet and ambient fluids in axisymmetric turbulent jets without heat release. Experiments by Ricou & Spalding (1961) confirmed that the equivalent diameter d^* in (8) and (9) provides the proper accounting for density effects in isothermal turbulent jets. This eliminated apparent differences in the scaling laws for non-reacting jets with matched and unmatched densities, and demonstrated that these could be unified in a single scaling law in terms of d^* in the absence of heat release.

3.2. *Observed effects of combustion heat release*

Burning jets of propane and hydrogen were briefly examined in the same investigation by Ricou & Spalding (1961). Their results showed a reduction of up to 30% in the mass entrainment rate of burning jets relative to the corresponding isothermal jets. Similar differences between isothermal and burning jets can be seen in the mean centreline velocities in figure 6 from measurements of Chigier & Strokin (1974), Takagi, Shin & Ishio (1981), and Muñiz & Mungal (1995) under conditions for which buoyancy effects are essentially negligible (e.g. Becker & Yamazaki 1978). In each case, the velocity in the burning jet decreases more slowly with x than in the non-burning jet under otherwise identical conditions. The lower rate of velocity decay is consistent with the reduced entrainment rate due to heat release noted by Ricou
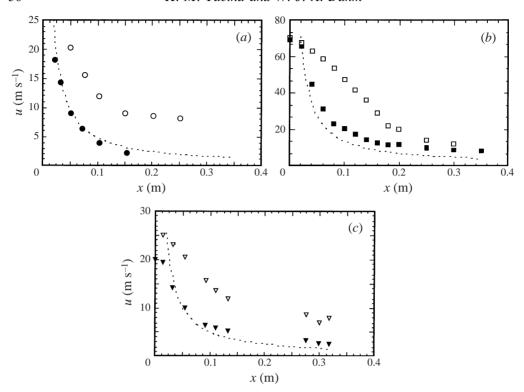
FIGURE 6. Comparisons of centreline velocity decay rates $u(x)$ in axisymmetric turbulent jets without heat release (solid symbols) and with combustion heat release (open symbols) under conditions for which buoyancy effects are negligible: (a) ●, ○, Chigier & Strokin (1974); (b) ■, □ Takagi *et al*, (1981); (c) ▼, ▽, Muñiz & Mungal (1995). Dashed lines are classical scaling for non-burning jets given in (7). Conditions for each case are given in table 1.

& Spalding. Such effects of heat release on velocity and conserved-scalar decay in jet flames have been noted since the earliest studies of Hawthorne *et al.* (1949), Thring & Newby (1953), Sunavala, Hulsa & Thring (1957) and Kremer (1967). Many studies have also noted the attendant increase in jet flame length over that which would be expected from the entrainment and mixing rate in non-burning jets (e.g. Eickhoff & Lenze 1969). Observations such as these have suggested that fundamental differences exist between burning and non-burning jets as a consequence of heat release effects (e.g. Beér & Chigier 1983).

3.3. *Application of the general equivalence principle*

Choosing X so that pure jet fluid corresponds to $X = 1$ as in figure 1, then for values of x sufficiently far upstream of the flame tip, the fluid in the jet is predominantly at $X > X_s$. In accordance with the equivalence principle in §2, we would extend the scaling laws for non-reacting turbulent jets from §3.1 to account for the effects of heat release by replacing ρ_∞ in (6)–(9) with $(\rho_\infty)_{eff}$ in (3b). The scaling laws for burning and non-burning axisymmetric turbulent jets should then be identical in the resulting 'extended momentum diameter' d^+ as

$$\delta = 0.44\,x \qquad (10a)$$

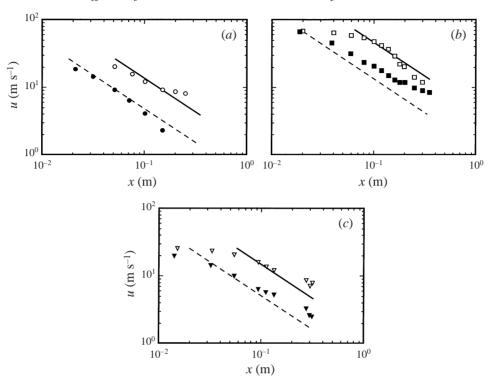$$u/u_0 = 6.5(x/d^+)^{-1}, \qquad (10b)$$

FIGURE 7. Comparisons of extended d^+ scaling law for $u(x)$ in §3 (lines) with data from figure 6 (symbols) for axisymmetric turbulent jets with and without combustion heat release under otherwise identical conditions, showing: $---$, scaling in (10b) without heat release; $\bullet, \blacksquare, \blacktriangledown$, data without heat release; ———, scaling in (10b) with heat release; $\bigcirc, \square, \triangledown$, data with heat release. See caption of figure 6. Conditions for each case are given in table 1.

where from (9)

$$d^+ \equiv (\rho_0/(\rho_\infty)_{eff})^{1/2} d_0 \qquad (11a)$$

or, in its more general form from (8),

$$d^+ \equiv \frac{2m_0}{(\pi(\rho_\infty)_{eff} J_0)^{1/2}}. \qquad (11b)$$

Note that $d^+ \equiv d^*$ for non-burning jets. The general equivalence principle of §2, when applied to axisymmetric turbulent jets, thus extends the classical scaling laws for non-burning jets to burning jets, and thereby unifies their scalings in terms of d^+ as did the classical momentum diameter d^* of Thring & Newby (1953) and Ricou & Spalding (1961) for non-burning jets with matched and unmatched densities.

Similarly, for values of x sufficiently far beyond the flame tip, fluid moving with the jet is at mole fractions $X < X_s$. In accordance with the equivalence principle in §2, the scaling laws applicable at such large x-values would be obtained by instead replacing ρ_0 in (6)–(9) with $(\rho_0)_{eff}$ in (4b). Thus (10a,b) would still apply, but the extended momentum diameter d^+ in that case becomes

$$d^+ \equiv \left((\rho_0)_{eff}/\rho_\infty\right)^{1/2} d_0. \qquad (12)$$

	Jet Fluid	u_0 (m s^{-1})	d_0 or h_0 (mm)	d^* or h^* (mm)	X_s	T_s (K)	$(T_\infty)_{eff}$ (K)	d^+ or h^+ (mm)
Barlow & Carter (1994)	H_2	288	3.75	0.98	0.296	2384	3259	3.25
Cheng et al. (1992)	H_2	680	2.0	0.53	0.296	2384	3259	1.73
Chigier & Strokin (1974)	CH_4	20	5.0	3.71	0.096	2226	2430	10.57
Flury & Schlatter (1995)	H_2	296	3.75	0.98	0.296	2384	3259	3.25
Flury & Schlatter (1995)	0.8 H_2 + 0.2 He	346	3.75	1.08	0.346	2324	3396	3.31
Flury & Schlatter (1995)	0.6 H_2 + 0.4 He	342	3.75	1.17	0.414	2228	3590	3.41
Muñiz & Mungal (1995)	0.4 CH_4 + 0.6 N_2	20	4.5	4.33	0.209	2075	2543	12.31
Rehm & Clemens (1996, 1998)	0.5 H_2 + 0.5 N_2	135	1.0	0.62	0.457	2025	3475	7.19
Takagi et al. (1981)	0.4 H_2 + 0.6 N_2	55	4.9	4.19	0.514	1872	3537	14.39

TABLE 1. Measurements used in §§3–5 for comparison with heat release effects predicted by the equivalence principle in §2, showing jet fluid composition (mole fractions), jet exit conditions, momentum diameter d^* (or width h^*), stoichiometric jet fluid mole fraction X_s, adiabatic flame temperature T_s, effective ambient fluid temperature $(T_\infty)_{eff}$ from (3a), and extended diameter d^+ (or width h^+) from (11a) or (22). Ambient fluid in all cases is air at $T_\infty \approx 300$ K. All cases correspond to essentially non-buoyant flames (e.g. Becker & Yamazaki 1978).

3.4. *Comparisons with experimental results*

The results in §3.3 suggest that the scaling laws for both non-burning and burning axisymmetric turbulent jets will be identical in terms of the extended momentum diameter d^+ in (11). Thus the mean centreline velocity for burning as well as non-burning jets would be given by (10b), and for burning jets yields a reduction in the velocity decay rate that depends on $(\rho_\infty)_{eff}/\rho_\infty$.

To assess the validity of the equivalence principle and the extended jet scaling laws that it implies, the result in (10b) is shown, for both burning and non-burning jets, by the lines in figure 7. The symbols give the data from figure 6 for burning and non-burning jets. Values of X_s and T_s, determined by the jet and ambient fluid compositions, are given for each case in table 1 together with the momentum diameter d^* for non-burning jets and d^+ for burning jets. Figure 7 shows that the agreement (solid line versus open symbols) for burning jets is about as good as the classical scaling of Thring & Newby (1953) and Ricou & Spalding (1961) is for non-burning jets (dashed line versus solid symbols).

In figure 7 and table 1 it is especially interesting to compare the effects of fuel dilution by Muñiz & Mungal (1995) with the pure fuel used by Chigier & Strokin (1974). The table shows that the dilution leads to significant differences in X_s and T_s, but the two effects offset each other (see figure 5) to give roughly the same $(T_\infty)_{eff}$. Indeed figures 7(a) and 7(c) suggest similar heat release effects in both cases, despite the dilution, with the differences between these cases being solely due to the different values of ρ_0. Furthermore, table 1 shows that dilution of the fuel by Takagi *et al.* (1981) produces even larger changes in X_s and T_s, leading in that case to a much higher $(T_\infty)_{eff}$, yet the agreement in figure 7(b) is equally as good as in the other two cases.

Figure 7 and table 1 also show that *ad hoc* use of T_s in place of $(T_\infty)_{eff}$, as has been proposed in some heuristic attempts to account for exothermicity in jets (e.g. Eickhoff & Lenze 1969), would lead to comparatively inaccurate prediction of heat release effects. This is clearest in the case of Takagi *et al.* (1981), where these temperatures differ by almost a factor of two (see figure 4b). The results in figure 7 suggest that d^+ in §3.3, based on the general equivalence principle in §2, appears to accurately predict the effect of heat release on the velocity decay in turbulent jets.

A further comparison is possible from the data of Flury & Schlatter (1995), who measured the centreline velocity decay in axisymmetric turbulent jet flames of hydrogen, diluted with various levels of helium, burning in air under conditions for which effects of buoyancy and coflow are negligible. Their results are compared with (10b) in figure 8, with relevant parameters in table 1. The classical isothermal scaling is shown by the dashed lines, and the solid lines give the present extended scaling for jets with heat release. For the burning jets, dilution changes both X_s and T_s. These again act to partly offset each other, but in this case produce an increase in $(T_\infty)_{eff}$ with increasing helium dilution. In each case, the net effect on the velocity decay in the burning jet is in good agreement with the extended scaling in (10b). Here, too, the differences between T_s and $(T_\infty)_{eff}$ are quite large. Note also that T_s, unlike $(T_\infty)_{eff}$, decreases with increasing dilution, and thus *ad hoc* methods based on substituting T_s for T_∞ would produce the opposite effect on the rate of velocity decay with increasing dilution from that obtained by the present equivalence principle.

All of these data for centreline velocity decay in both burning and non-burning jets are shown in terms of (x/d^+), as indicated by (10b), in figure 9. The agreement with the extended scaling in the far field, shown by the solid line, is equally good for the
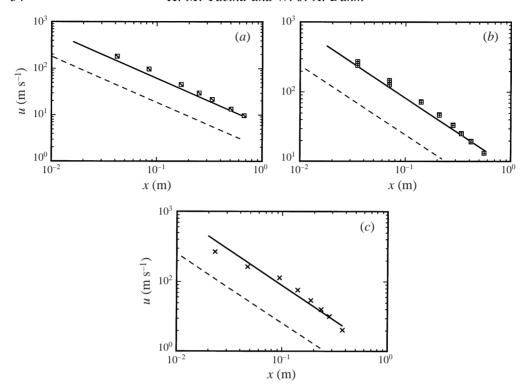
FIGURE 8. Comparisons of extended d^+ scaling law for $u(x)$ in §3 (lines) with data of Flury & Schlatter (1995) (symbols) for axisymmetric turbulent jet flames of hydrogen with various levels of helium dilution, under conditions for which buoyancy effects are negligible. — — —, Scaling in (10b) without heat release; ——, scaling in (10b) with heat release; (*a*) data for 0% helium dilution □ (*b*), 20% helium dilution ⊞; (*c*) 40% helium dilution ×. Conditions for each case are given in table 1. Dashed lines are equivalent to the classical d^* scaling of Thring & Newby (1953) and Ricou & Spalding (1961) for non-exothermic jets.

burning and non-burning jets, indicating that the general equivalence principle in §2 appears to correctly extend the scaling laws for density effects in non-burning jets to predict the effects of heat release in turbulent jet flames.

Moreover, since the scaling for $\delta(x)$ in (10a) does not depend on either the jet or ambient fluid densities, the equivalence principle implies that, in the absence of significant buoyancy, there will be no effect of heat release on the flow width. To test this, figure 10 shows data for $\delta(x)$ from burning and non-burning axisymmetric turbulent jets, together with the far-field scaling in (10a). The agreement with data from burning jets is again about as good as that between non-burning jets and the classical scaling, in agreement with the equivalence principle in §2.

The mass flux scaling $m(x) \sim \rho_\infty u(x)\delta^2(x)$, and thus the entrainment rate $\mathrm{d}m/\mathrm{d}x$, are obtained from the centreline velocity and flow width scalings. As a consequence, the centreline conserved-scalar decay follows as $\zeta(x) \sim m_\zeta/m(x)$, where m_ζ is the mass flux of scalar from the jet source. For non-burning jets it is popular to write this in terms of an 'exit-scalar value' $\zeta_0 \equiv (m_\zeta/m_0)$ as

$$\zeta/\zeta_0 = 5.4(x/d^*)^{-1}, \tag{13}$$

where the constant is from Dahm & Dimotakis (1990). From the equivalence principle, this scaling is extended to both burning and non-burning jets by replacing ρ_∞ with
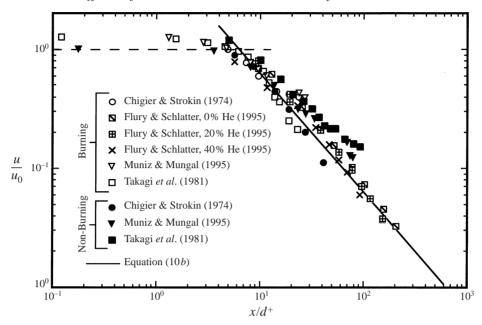
FIGURE 9. Comparison of data from figures 6–8 for non-burning jets (solid symbols) and burning jets (open symbols) with the unified far-field scaling law in (10*b*) (solid line) for outer velocity scale $u(x)$ in axisymmetric turbulent jets with and without combustion heat release. For jets without heat release, d^+ scaling becomes identical to classical d^* scaling in (7) of Thring & Newby (1953) and Ricou & Spalding (1961). Note that the agreement of the present d^+ scaling with data from burning jets is comparable to that of classical d^* scaling with data from non-burning jets. Dashed line gives near-field scaling in § 5.

$(\rho_\infty)_{eff}$, giving

$$\zeta/\zeta_0 = 5.4(x/d^+)^{-1}. \tag{14}$$

To test this, figure 11 compares the centreline conserved-scalar decay $\zeta(x)$ measured in non-buoyant turbulent jet flames and in turbulent jets without heat release, where the solid line gives the unified scaling in (14). The agreement of data from both burning and non-burning jets with this scaling further supports the general equivalence principle in § 2.

Finally, from the conserved-scalar scaling above, the flame length L in burning jets is determined by the downstream distance x at which the maximum scalar value, which scales with $\zeta(x)$, reaches the stoichiometric value ζ_s. Thus from (14)

$$L/d^+ = 10(\varphi + 1), \tag{15}$$

where φ is the mass ratio of ambient-to-jet fluid in a stoichiometric mixture, and the constant is from isothermal measurements of Dahm & Dimotakis (1987). From (15), the flame lengths of burning jets would thus be longer than those indicated by mixing in isothermal jets by the factor $d^+/d^* = [(T_\infty)_{eff}/T_\infty]^{1/2}$. As table 1 reveals, this ratio is typically about 3 for most hydrocarbon fuels and for a wide range of dilutions. The result in (15) is in good agreement with available flame length data from non-buoyant turbulent jet diffusion flames (e.g. see figures 1 and 2 of Blake & McDonald 1993, for which the equivalence in § 2 and the extremely small values of X_s justify their *ad hoc* use of T_s in place of $(T_\infty)_{eff}$).
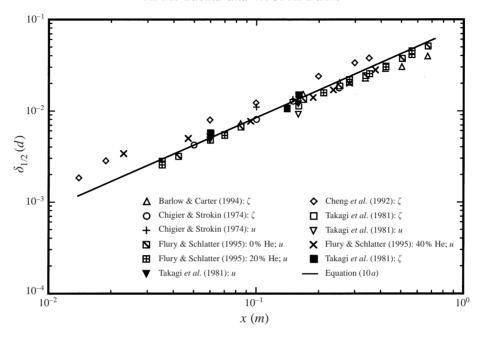
FIGURE 10. Comparison of outer length scale $\delta(x)$ from mean profiles of velocity u and conserved scalar ζ measured in axisymmetric turbulent jets with (open symbols) and without (solid symbols) combustion heat release under conditions for which buoyancy effects are negligible. Solid line gives $\delta_{1/2} = 0.08x$, from δ in (10a) and Gaussian profile shape. As in figure 9, agreement of data from burning jets with the unified scaling in §3.3 is comparable to that from jets without heat release.
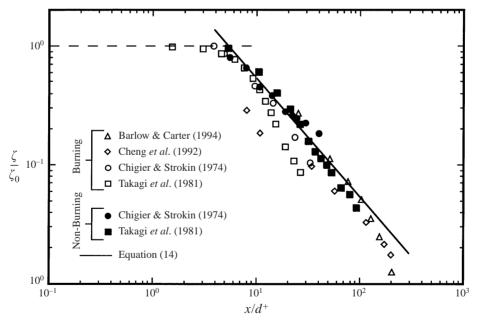

FIGURE 11. Comparison of data from non-burning jets (solid symbols) and burning jets (open symbols) with unified far-field scaling law in (14) (solid line) for centreline conserved-scalar decay $\zeta(x)$ in axisymmetric turbulent jets with and without combustion heat release. Dashed line gives near-field scaling in §5.

4. Heat release effects in planar turbulent jets

The equivalence in §2 gives the effects of heat release on the outer-variable scaling laws for any turbulent shear flow. In this section we apply it to planar turbulent jets. Rehm & Clemens (1996, 1998) have experimentally documented effects of heat release due to burning in planar turbulent jets issuing from a slot of width h under conditions for which buoyancy effects are negligible. Their data provide a further opportunity to assess the validity of the general principle proposed here for equivalence in the scaling laws of non-burning and burning flows, and to assess the accuracy of the heat release effects predicted by this principle.

4.1. *Scaling laws for non-reacting planar jets*

From dimensional considerations, the outer variables $\delta(x)$ and $u(x)$ in the self-similar far field of non-reacting planar turbulent jets scale with the jet source momentum flux per unit span J_0 and the ambient fluid density ρ_∞ as

$$\delta \sim x, \tag{16a}$$

$$u \sim (J_0/\rho_\infty)^{1/2} x^{-1/2} \tag{16b}$$

(e.g. Gutmark & Wygnanski 1976). As in §3.1, it is common to write this in terms of a far-field equivalent slot width h^* as

$$u/u_0 \sim (x/h^*)^{-1/2}, \tag{17}$$

where

$$h^* \equiv m_0^2/(\rho_\infty J_0). \tag{18}$$

For jets issuing with uniform density and velocity, (18) reduces to

$$h^* = (\rho_0/\rho_\infty) h_0, \tag{19}$$

where h_0 is the physical slot width and ρ_0 is the jet fluid density. These outer-variable scalings then set the far-field scaling for the mass flux per unit span as $m(x) \sim \rho_\infty u(x)\delta(x)$, with the centreline conserved scalar then following as $\zeta(x) \sim m_\zeta/m(x)$. For non-reacting planar turbulent jets this gives

$$\zeta/\zeta_0 = 5.4(x/h^*)^{-1/2}, \tag{20}$$

where the scaling constant comes from experimental data.

4.2. *Application of the general equivalence principle*

Defining X so that pure jet fluid corresponds to $X = 1$ as in figure 1, then at values of x sufficiently upstream of the flame tip the fluid in the jet is predominantly at $X > X_s$. Accordingly the equivalence principle in §2 indicates that the scalings in §4.1 for the non-burning jet can be extended to burning jets by replacing ρ_∞ in (16)–(20) with $(\rho_\infty)_{eff}$ in (3b). Thus the scaling for the centreline conserved scalar in (20) becomes

$$\zeta/\zeta_0 = 5.4(x/h^+)^{-1/2}, \tag{21}$$

with h^+ from (19) becoming

$$h^+ = (\rho_0/(\rho_\infty)_{eff}) h_0. \tag{22}$$

The scaling laws for both non-burning and burning jets should be identical in terms of h^+. Following the same reasoning as in §3.4, the flame length L in this case scales as
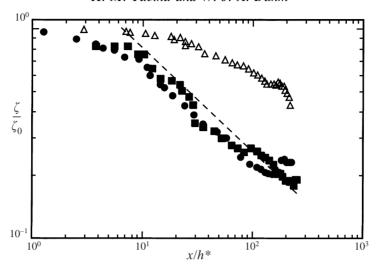
FIGURE 12. Comparison of centreline conserved-scalar decay $\zeta(x)$ in planar turbulent jets without heat release (solid symbols) and with heat release (open symbols) in terms of classical momentum width h^* of §4.1, under conditions for which buoyancy effects are negligible. Dashed line is h^* scaling in (20) for non-burning jets. Data from Rehm & Clemens (1996, 1998). ■, He jet; ●, He/N$_2$ jet; △, H$_2$/N$_2$ jet flames. Conditions are as given in table 1. The same data are compared in figure 13 in the extended momentum width h^+ of §4.2.
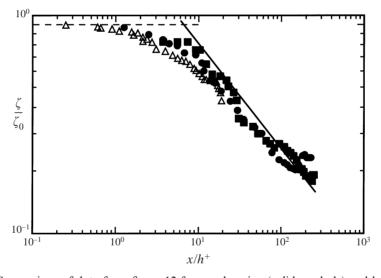

FIGURE 13. Comparison of data from figure 12 for non-burning (solid symbols) and burning (open symbols) planar turbulent jets with the unified far-field scaling law in (21) (solid line). For jets without heat release, h^+ scaling becomes identical to classical h^* scaling in figure 12. The agreement of the present h^+ scaling with far-field data from the burning jet is comparable to that of classical h^* scaling with data from the non-burning jets. Dashed line gives near-field scaling in §5.

$$L/h^+ \sim (\varphi + 1)^2. \tag{23}$$

Note that, owing to the different exponents in (11a) and (22), the effect of heat release on flame length is far more pronounced in planar jets than in axisymmetric jets.

4.3. *Comparisons with experimental results*

Figure 12 shows the data of Rehm & Clemens (1996, 1998) for the centreline conserved-scalar decay in burning and non-burning planar turbulent jets in the classical equivalent slot width h^* in (18) and (19). Results for the two non-burning jets, which have different values of ρ_0, show good agreement in the classical h^* scaling in (20). In contrast, results from the burning jet show a much lower rate of mixing, and do not appear consistent with the h^* scaling that governs the non-reacting flow.

However, when these same data are plotted as in (21), in terms of h^+, then the results for the burning and non-burning jets are seen in figure 13 to follow the same scaling, in agreement with the equivalence principle in §2, where the solid line gives the far-field scaling in (21). The agreement of the present h^+ scaling with data from the burning jet is comparable to that of the classical h^* scaling with the data from the non-burning jets. In this form the data from the burning jet can be seen to just barely reach the far field. Even in the transition region, the data from the burning and non-burning jets, when scaled by h^+, appear to be in agreement.

We conclude that the equivalence principle in §2 accurately predicts the effects of combustion heat release on the outer-variable scalings in planar turbulent jets, as it did for axisymmetric turbulent jets in §3, under conditions for which buoyancy effects are negligible.

5. Heat release effects on jet near-field length

The scaling laws for turbulent jets in §3 and §4 apply in the far field, at values of x sufficiently large that the only remaining dynamically relevant aspect of the jet source is its momentum flux, which remains invariant when buoyancy effects are negligible. By contrast the near field, or potential core region, refers to values of x sufficiently small that the centreline velocity $u(x)$ and conserved scalar $\zeta(x)$ remain essentially constant at their source values u_0 and ζ_0. The transition from this near-field scaling to the far-field scaling in (14) and (21) can be seen, for example, in figures 9, 11 and 13. The length l of the near field can thus be associated with the point at which the two scalings cross, and is known to be affected by heat release. For example, Savaş & Gollahalli (1986) and Clemens & Paul (1995) have shown dramatic differences in the potential core region of burning and non-burning axisymmetric turbulent jets under otherwise identical conditions. Their results indicate a large increase in the length of the near field under burning conditions, and striking changes in the vortical structure of the potential core region (e.g. see figures 1(a, b) of Savaş & Gollahalli 1986).

These changes in the near field due to heat release are probably a result of several factors, some of which were noted in §1 and are discussed in detail by Savaş & Gollahalli and by Clemens & Paul. However, here we note that, owing to the universality of the jet scalings in (14) or (21), the transition between the near- and far-field scalings must occur at the fixed value $(l/d^+) = 5.4$, or $(l/h^+) = 5.4$, irrespective of the level of heat release. For axisymmetric turbulent jets, the resulting near-field length becomes

$$l/d^* = 5.4\left((T_\infty)_{eff}/T_\infty\right)^{1/2}, \tag{24}$$

while for planar turbulent jets this becomes

$$l/h^* = 5.4\left((T_\infty)_{eff}/T_\infty\right). \tag{25}$$

Note that (24) and (25) indicate an increase in the length of the near field due to heat release, with the effect being more pronounced for planar jet flames.

For axisymmetric turbulent jet flames formed by typical hydrocarbon fuels issuing into air, values of $(T_\infty)_{eff}$ such as in table 1 indicate that the near field will typically be about 3 times longer in burning jets than in non-burning jets. This result, from (24), agrees with the available qualitative observations in axisymmetric jets of Yule *et al.* (1981), Savaş & Gollahalli (1986), and Clemens & Paul (1995), and is further supported by the quantitative agreement evident in the transition region in figure 9 between data from burning jets (open symbols) and non-burning jets (solid symbols). Similarly, from (25) and table 1, in planar turbulent jets the predicted effect of heat release on the near-field length is an increase by typically about a factor of 10, which is also seen to be in good quantitative agreement in figures 12 and 13 with the data of Rehm & Clemens (1996, 1998) from burning and non-burning jets.

The increased near-field lengths due to heat release in (24) and (25) require an attendant reduction in the growth rate of the mixing layer on the jet periphery in the near field. This in turn implies changes in the vortex size and spacing within the mixing layer that are also qualitatively consistent with the effects seen due to heat release in figures 1(*a*, *b*) of Savaş & Gollahalli (1986) and in figures 5 and 7 of Clemens & Paul (1995).

We conclude that the simple equivalence principle in §2 correctly predicts the dominant observed effects of heat release on the length and vortex structure of the near fields of planar and axisymmetric turbulent jet flames. It must be cautioned, however, that there are likely to be other effects of heat release that may play an additional role in setting details of the vortex size and structure in the near field jets (e.g. Yamashita, Kushida & Takeno 1990; Takeno 1994).

6. Concluding remarks

The equivalence introduced here, based on the principle in figure 5, accounts for the effects of heat release on turbulent shear flows through the scaling laws for the local outer variables that govern the corresponding non-reacting flow. Its application is restricted to conditions under which buoyancy effects are negligible. Under such conditions, the results in §3–5 indicate that the heat release mechanism considered here is the principal effect of exothermicity on the outer-variable scalings in most turbulent reacting flows. This equivalence principle was seen here to accurately predict the dominant heat release effects, in both the near and far fields, of planar and axisymmetric turbulent jet flames over a range of fuels and dilutions.

This general principle (see also Tacina & Dahm 1996) is based on the piecewise linear form of $T(X)$ in the mole fraction X, which is demanded by enthalpy conservation in a reacting flow under the conditions noted in §2. Since a linear $T(X)$ is indicative of simple fluid mixing, without reaction, it is apparent that on either side of the stoichiometric mole fraction X_s, the temperature field $T(X)$ in the reacting flow is equivalent to that which would occur in a corresponding non-reacting flow with the temperature of one of the fluids raised to a fictitious elevated value given here. This is done in practice by replacing one of the two fluid densities in the outer-variable scaling laws for the corresponding non-reacting flow with the effective value given in (3*b*) or (4*b*) that corresponds to this elevated temperature. The density field $\rho(x, t)$ in the fictitious non-reacting flow will then be identical to that which occurs in the exothermic reacting flow wherever the mole fraction field $X(x, t)$ is above (or below) the stoichiometric value X_s. In this manner, the dominant effects of density

changes due to heat release in the exothermic flow are obtained from the scaling of the non-reacting flow.

Application of this principle was demonstrated for axisymmetric turbulent jets in §3. In that case it led to a generalized momentum diameter d^+ that extends the classical Thring & Newby (1953) and Ricou & Spalding (1961) momentum diameter d^* to exothermic flows. In terms of (x/d^+), the scaling laws for the outer variables u and δ in jets with and without heat release become identical. For values of x sufficiently smaller than the flame length, d^+ is obtained from d^* by replacing ρ_∞ with $(\rho_\infty)_{eff}$. Doing so was seen in figures 7–11 to accurately predict the reduction in entrainment and mixing rates observed due to heat release in turbulent jet flames for a variety of fuels and dilutions. These, in turn, determine the effect of heat release on the flame length as noted in (15). Similarly, when this equivalence principle was applied to planar turbulent jets in §4, it led to an extended momentum width h^+ that from figures 12 and 13 was seen to correctly predict the much stronger effect of heat release on the entrainment and mixing rate in that flow as well, with the effect on planar turbulent jet flame lengths given in (23).

Application of the equivalence principle also led to the observation that the near-field length (l/d^+), or (l/h^+), must scale with the point at which the near- and far-field scalings cross, as in figures 9, 11 and 13. This led to the results in (24) and (25) for the effect of heat release on the near-field length, which indicate a much larger increase due to heat release in planar turbulent jets than is the case for axisymmetric jets. The results were found to be in good agreement with available observations and measurements in the transition region of both planar and axisymmetric turbulent jet flames.

While this equivalence principle explains most observed effects of heat release, it will of course fail if used outside the range over which its physical assumptions apply. Most obvious among these is when buoyancy due to heat release is no longer negligible, and under such conditions the method is not meant to be applied. The same is true when the increase in viscosity due to heat release produces a sufficient reduction in Reynolds number for the flow to become transitional or laminar (e.g. Takeno 1994). Near the flame tip, where mole fractions are centred around the stoichiometric value X_s, the local mole fraction field $X(x, t)$ is not dominated by either of the linear branches of $T(X)$ and the underlying equivalence then also fails. Similarly, when the underlying adiabatic assumption is sufficiently violated that the temperature is no longer adequately determined by the mole fraction, as could potentially occur in very strongly radiating flows, or in flows with large heat extraction, then the method is not meant to be applied. A similar limitation could apply if differential diffusion effects are sufficiently pronounced that the temperature is no longer adequately determined by the mole fraction. If the reactions are not sufficiently fast to avoid significant chemical non-equilibrium effects, as might occur in very high-speed flows where local extinction effects can be significant, then the temperature field will no longer be simply determined by the mole fraction, and the method should not be applied. Finally, if temperatures in the reacting flow are high enough for dissociation effects to become significant, such as can occur in oxygen-enriched combustion, then $T(X)$ will no longer be piecewise linear. However, in most practical combustion applications, the equivalence principle will be applicable and appears to capture the dominant effects of heat release on the outer variables, and thus the resulting entrainment and mixing properties, of turbulent shear flows.

Although the notion of extending the scaling laws for non-reacting flows to account for heat release effects by a change in ambient fluid density is not entirely new,

Fuel	Oxidizer	X_s	MW_s	$(MW_\infty)_{eff}$	$\dfrac{(MW_\infty)_{eff}}{MW_\infty}$	$\dfrac{(T_\infty)_{eff}}{T_\infty}$
H_2	Air	0.296	24.3	33.6	1.2	10.9
$0.8\ H_2 + 0.2\ He$	Air	0.346	22.7	33.4	1.2	11.3
$0.6\ H_2 + 0.4\ He$	Air	0.414	20.6	33.0	1.1	12.0
$0.5 H_2 + 0.5\ Ne$	Air	0.457	25.4	34.2	1.2	11.6
$0.4\ H_2 + 0.6\ Ne$	Air	0.514	25.7	34.2	1.2	11.8
CH_4	Air	0.096	27.4	28.7	1.0	8.1
$0.4\ CH_4 + 0.6\ N_2$	Air	0.209	27.6	28.8	1.0	8.5

TABLE 2. Comparison of relative effects of molecular weight ratio and temperature ratio on effective density in (A 1). Shown for each fuel and oxidizer are the stoichiometric jet fluid mole fraction X_s, molecular weight of stoichiometric products MW_s, effective molecular weight $(MW_\infty)_{eff}$ of ambient fluid from (A 2), and molecular weight and temperature ratios in (A 1). Oxidizer in all cases is at $T_\infty \approx 300\,K$. Note that the influence of molecular weight changes on the effective density $(\rho_\infty)_{eff}$ in (A 1) is typically small compared to the effect of temperature rise due to heat release, as assumed in §2.3.

previous attempts to do so have lacked the rigorous basis developed here. Hawthorne *et al.* (1949) noted the lower entrainment rate in burning jets in the absence of buoyancy, and thus used T_s in place of T_∞ in their expression for flame lengths in an attempt to account for this. After noting the errors that result when applying the isothermal density correction of Thring & Newby (1953) to turbulent jet flames, several studies have similarly advocated heuristically treating a jet flame as a cold, high-density jet entraining hot, low-density ambient gases at the flame temperature T_s (e.g. Rhine & Tucker 1991). That *ad hoc* approach bears some resemblance to the formal result obtained here by applying the general equivalence principle of §2 to turbulent jets, but differs in the simplistic way in which it assigns the fictitious ambient fluid temperature. Moreover it lacks the generality or rigorous basis that comes from the fundamental equivalence in figure 5. Accordingly, when the stoichiometric mole fraction is not small, as in some of the cases in table 1, the predictions obtained with such previous heuristic approaches can significantly underestimate the effects of heat release. Furthermore, as noted in §3.4, the *ad hoc* use of T_s in place of T_∞ in some circumstances even predicts the opposite effects of heat release from those predicted by the present equivalence principle, as in the case of increasing helium or nitrogen dilution of hydrogen fuel burning in air.

Appendix

It is assumed throughout that the effective densities are changed from their true values by the temperature rise due to heat release, and that molecular weight changes due to chemical transformations have a comparatively negligible effect. It may be

readily shown that this is valid for all cases in table 1. Considering an ideal gas and constant pressure, the effective density is related to the effective temperature and molecular weight as

$$(\rho_\infty)_{eff} = \rho_\infty \left(\frac{T_\infty}{(T_\infty)_{eff}} \right) \left(\frac{(MW_\infty)_{eff}}{MW_\infty} \right), \tag{A1}$$

where, following the same approach that yields the effective temperature, the effective molecular weight is given by

$$(MW_\infty)_{eff} = MW_s - \frac{X_s}{1 - X_s}(MW_0 - MW_s), \tag{A2}$$

with subscripts following the notation in §3 and §4. For each of the cases in table 1, adiabatic equilibrium calculations provide MW_s and thus allow the relative effects of the temperature ratio and molecular weight ratio in (A1) to be determined. Results for each case are shown in table 2, where it can be seen that the effective molecular weight ratio remains near unity, while the effective temperature ratio is typically an order of magnitude larger. In view of this, the present assumption appears clearly justified.

REFERENCES

BARLOW, R. S. & CARTER, C. D. 1994 Raman/Rayleigh/LIF measurements of nitric oxide formation in turbulent hydrogen jet flames. *Combust. Flame* **97**, 261–280.

BECKER, H. A. & YAMAZAKI, S. 1978 Entrainment, momentum flux and temperature in vertical free turbulent jet diffusion flames. *Combust. Flame* **33**, 123–149.

BEÉR, J. M. & CHIGIER, N. A. 1983 *Combustion Aerodynamics.* Robert E. Krieger Publ., Malabar, FL.

BLAKE, T. R. & MCDONALD, M. 1993 An examination of flame length data from vertical turbulent diffusion flames. *Combust. Flame* **94**, 426–432.

CHENG, T. S., WEHRMEYER, J. A. & PITZ, R. W. 1992 Simultaneous temperature and multispecies measurements in a lifted hydrogen diffusion flame. *Combust. Flame* **91**, 323–345.

CHIGIER, N. A. & STROKIN, V. 1974 Mixing process in a free turbulent diffusion flame. *Combust. Sci. Tech.* **9**, 111–118.

CLEMENS, N. T. & PAUL, P. H. 1995 Effects of heat release on the near field structure of hydrogen jet diffusion flames. *Combust. Flame* **102**, 271–284.

DAHM, W. J. A. & DIMOTAKIS, P. E. 1987 Measurements of entrainment and mixing in turbulent jets. *AIAA J.* **25**, 1216–1223.

DAHM, W. J. A. & DIMOTAKIS, P. E. 1990 Mixing at large Schmidt number in the self-similar far field of turbulent jets. *J. Fluid Mech.* **217**, 299–330.

EICKHOFF, H. & LENZE, B. 1969 Grundformen von Strahlflammen. *Chemie Ingeniuer Technik* **20**, 1095–1099.

FLURY, M. & SCHLATTER, M. 1995 Experimental and numerical investigation of turbulent non-premixed hydrogen flames. 1995 *Joint Meeting of the German and French Sections.* The Combustion Institute, Pittsburgh.

GÜNTHER, R. & LENZE, B. 1966 Die Länge von Diffusions-Strahlflammen. *Gaswärme* **15**, 376–381.

GUTMARK, E. & WYGNANSKI, I. 1976 The planar turbulent jet. *J. Fluid Mech.* **73**, 465–495.

HAWTHORNE, W. R., WEDDEL, D. S. & HOTTEL, H. C. 1949 Mixing and combustion in turbulent gas jets. *Proc. 3rd Intl Symp. on Combustion, Flame, and Experimental Phenomena*, pp. 266–288. Williams & Wilkins, Co., Baltimore.

HOTTEL, H. C. & HAWTHORNE, W. R. 1949 Diffusion in laminar flame jets. *Proc. 3rd Intl Symp. on Combustion, Flame, and Experimental Phenomena*, pp. 254–266, Williams & Wilkins, Co., Baltimore.

KREMER, H. 1967 Mixing in a plane free-turbulent-jet diffusion flame. *Proc. 11th Intl Symp. on Combustion*, pp. 799-806. The Combustion Institute, Pittsburgh.

MUÑIZ, L. & MUNGAL, M. G. 1995 A PIV investigation of turbulent diffusion flames. *Paper* WSS/CI-95F-206, *1995 Fall Mtg., Western States Section of the Combustion Institute.* The Combustion Institute, Pittsburgh.

REHM, J. E. & CLEMENS, N. T. 1996 The structure of planar hydrogen jet diffusion flames. *AIAA Paper* 96-0704.

REHM, J. E. & CLEMENS, N. T. 1998 The large-scale turbulent structure of nonpremixed planar jet flames. *Combust. Flame* **116**, 615–626.

RHINE, J. M. & TUCKER, R. J. 1991 *Modelling of Gas-Fired Furnaces and Other Industrial Heating Processes.* McGraw-Hill.

RICOU, F. P. & SPALDING, D. B. 1961 Measurements of entrainment and mixing by axisymmetrical turbulent jets. *J. Fluid Mech.* **11**, 21–32.

SAVAŞ, O. & GOLLAHALLI, S. R. 1986 Flow structure in near-nozzle region of gas jet flames. *AIAA J.* **24**, 1137–1140.

SUNAVALA, P. D., HULSA, C. & THRING, M. 1957 Mixing and combustion in free and enclosed turbulent jet diffusion flames. *Combust. Flame* **1**, 179–193.

TACINA K. M. & DAHM, W. J. A. 1996 Heat release effects on scaling laws for turbulent shear flows. *Bull. Am. Phys. Soc.* **41** (9), 1814 (abstract only).

TAKAGI, T., SHIN, H.-D. & ISHIO, A. 1981 Properties of turbulence in turbulent diffusion flames. *Combust. Flame* **40**, 121–140.

TAKENO, T. 1994 Transition and structure of jet diffusion flames. *Proc. 25th Intl. Symp. on Combustion*, pp. 1061-1073. The Combustion Institute, Pittsburgh.

THRING, M. W. & NEWBY, M. P. 1953 Combustion length of enclosed turbulent jet flames. *Proc. 4th Intl. Symp. on Combustion*, pp. 789-796, Williams & Wilkins, Co., Baltimore.

WYGNANSKI, I. & FIEDLER, H. 1969 Some measurements in the self-preserving jet. *J. Fluid. Mech.* **38**, 577–612.

YAMASHITA, H., KUSHIDA, G. & TAKENO, T. 1990 A numerical study of the transition of jet diffusion flames. *Proc. R. Soc. Lond.* A **431**, 301.

YULE, A. J., CHIGIER, N. A., RALPH, S., BOULDERSTONE, R. & VENTURA, J. 1981 Combustion-transition interaction in a jet flame. *AIAA J.* **19**, 752–760.